Nrf2 acts cell-autonomously in endothelium to regulate tip cell formation and vascular branching

Yanhong Wei[a], Junsong Gong[a], Rajesh K. Thimmulappa[b], Beata Kosmider[c], Shyam Biswal[b], and Elia J. Duh[a,1]

[a]Department of Ophthalmology, The Johns Hopkins University School of Medicine, Baltimore, MD 21287; [b]Department of Environmental Health Sciences, Bloomberg School of Public Health, Johns Hopkins University, Baltimore, MD 21205; and [c]Department of Medicine, National Jewish Health, Denver, CO 80206

Edited* by Jeremy Nathans, Johns Hopkins University, Baltimore, MD, and approved August 28, 2013 (received for review May 16, 2013)

Angiogenesis, in which new blood vessels form via endothelial cell (EC) sprouting from existing vessels, is a critical event in embryonic development and multiple disease processes. Many insights have been made into key EC receptors and ligands/growth factors that govern sprouting angiogenesis, but intracellular molecular mechanisms of this process are not well understood. NF-E2–related factor 2 (Nrf2) is a transcription factor well-known for regulating the stress response in multiple pathologic settings, but its role in development is less appreciated. Here, we show that Nrf2 is increased and activated during vascular development. Global deletion of Nrf2 resulted in reduction of vascular density as well as EC sprouting. This was also observed with specific deletion of Nrf2 in ECs, but not with deletion of Nrf2 in the surrounding nonvascular tissue. Nrf2 deletion resulted in increased delta-like ligand 4 (Dll4) expression and Notch activity in ECs. Blockade of Dll4 or Notch signaling restored the vascular phenotype in Nrf2 KOs. Constitutive activation of endothelial Nrf2 enhanced EC sprouting and vascularization by suppression of Dll4/Notch signaling in vivo and in vitro. Nrf2 activation in ECs suppressed Dll4 expression under normoxia and hypoxia and inhibited Dll4-induced Notch signaling. Activation of Nrf2 blocked VEGF induction of VEGFR2-PI3K/Akt and downregulated HIF-2α in ECs, which may serve as important mechanisms for Nrf2 inhibition of Dll4 and Notch signaling. Our data reveal a function for Nrf2 in promoting the angiogenic sprouting phenotype in vascular ECs.

Angiogenesis is a critical event in embryonic development and multiple disease processes, including tumorigenesis, proliferative diabetic retinopathy, atherosclerosis, and peripheral arterial disease (1). Angiogenesis is initiated by endothelial cell (EC) sprouting, which is driven and guided by a VEGF gradient. The specification of endothelial tip and stalk cells, prominently regulated by delta-like 4 (Dll4)/Notch signaling, is a major control point in EC sprouting (2, 3). The tip and stalk cell phenotypes are dynamic, and precise modulation of sprouting and branching patterns is crucial in angiogenesis (4). However, the mechanisms regulating this process are still not completely clear.

NF-E2–related factor 2 (Nrf2) is a ubiquitous transcription factor induced by endogenous and exogenous stressors (5). Nrf2 is normally sequestered in the cytoplasm and targeted for ubiquitination by its repressor, Kelch-like ECH-associated protein 1 (Keap1). Upon activation, Nrf2 is released from Keap1 and translocates into the nucleus to activate the transcription of multiple cytoprotective genes. Nrf2 is known to play a critical role in many disease settings, offering a mechanism for cellular protection (5). Oncogene-induced Nrf2 transcription was found to promote tumorigenesis by enhancing detoxification in cancer cells (6). Apart from cytoprotection, recent studies showed that Nrf2 contributes to cancer development by modulating metabolic activities (7) and maintenance of hematopoietic stem cell function by regulating quiescence and self-renewal (8), implicating a role of Nrf2 in multiple cellular processes. Although Nrf2 plays a critical role in multiple pathologic settings, very little attention has been devoted to its role in regulating basic physiologic processes during development.

Nrf2 has been found to regulate angiogenesis, but the role of Nrf2 in angiogenesis in vivo is context-dependent. Knockdown of Nrf2 contributes to the suppression of colon tumor angiogenesis (9), whereas deletion of Nrf2 leads to exacerbation of ischemia-induced angiogenesis in limbs and lung (10, 11). The effect of Nrf2 in these settings is likely related, in part, to its influence on the levels of angiogenic factors in the tissue milieu.

Although Nrf2 appears to play a regulatory role in angiogenesis, the cellular context of Nrf2's effects remain to be determined, as well as the underlying intracellular mechanisms. Here, by using genetic loss of function (LOF) and gain of function (GOF), we find that Nrf2 promotes angiogenic sprouting and vascular branching in an EC-autonomous manner. Based on in vivo, ex vivo, and in vitro experiments, we identify that suppression of Dll4 and Notch signaling contributes to the enhanced sprouting capacity of ECs with Nrf2 activation. Together, these results reveal that Nrf2 is a critical intracellular regulator of ECs governing angiogenic sprouting and implicate a unique function of Nrf2 in regulating angiogenesis.

Results

Genetic Ablation of *Nrf2* Reduces Angiogenic Sprouting and Vascular Density. To determine the importance of Nrf2 during sprouting angiogenesis, we investigated developmental angiogenesis in the retina in *Nrf2*-deficient mice ($Nrf2^{-/-}$) at postnatal day (P) 5. $Nrf2^{-/-}$ retinas exhibited reduced tip cells and filopodia projections, branch points, and vascular density (Fig. 1 *A*–*E*), whereas no significant change was observed in length of vasculature extensions (Fig. S1*A*). The in vivo EC proliferation assay (BrdU incorporation assay) showed a decreased number of $BrdU^+$ ECs

Significance

Angiogenesis, in which new blood vessels form via endothelial cell (EC) sprouting from existing vessels, is critical in embryonic development and multiple disease processes. The intracellular molecular mechanisms governing sprouting angiogenesis remain incompletely understood. We found that transcription factor NF-E2–related factor 2 (Nrf2), well-known for regulating the stress response in multiple pathologic settings, is a critical intracellular regulator in ECs for sprouting angiogenesis in vascular development through delta-like 4 (Dll4)/Notch signaling. Understanding the molecular mechanisms by which Nrf2 regulates angiogenesis could facilitate therapeutic strategies targeting Nrf2 to treat angiogenesis-related diseases, including tumorigenesis, proliferative diabetic retinopathy, atherosclerosis, and ischemic disorders.

Author contributions: Y.W. and E.J.D. designed research; Y.W. and J.G. performed research; R.K.T., B.K., and S.B. contributed new reagents/analytic tools; Y.W., J.G., and E.J.D. analyzed data; and Y.W. and E.J.D. wrote the paper.

The authors declare no conflict of interest.

*This Direct Submission article had a prearranged editor.

[1]To whom correspondence should be addressed. E-mail: eduh@jhmi.edu.

This article contains supporting information online at www.pnas.org/lookup/suppl/doi:10.1073/pnas.1309276110/-/DCSupplemental.

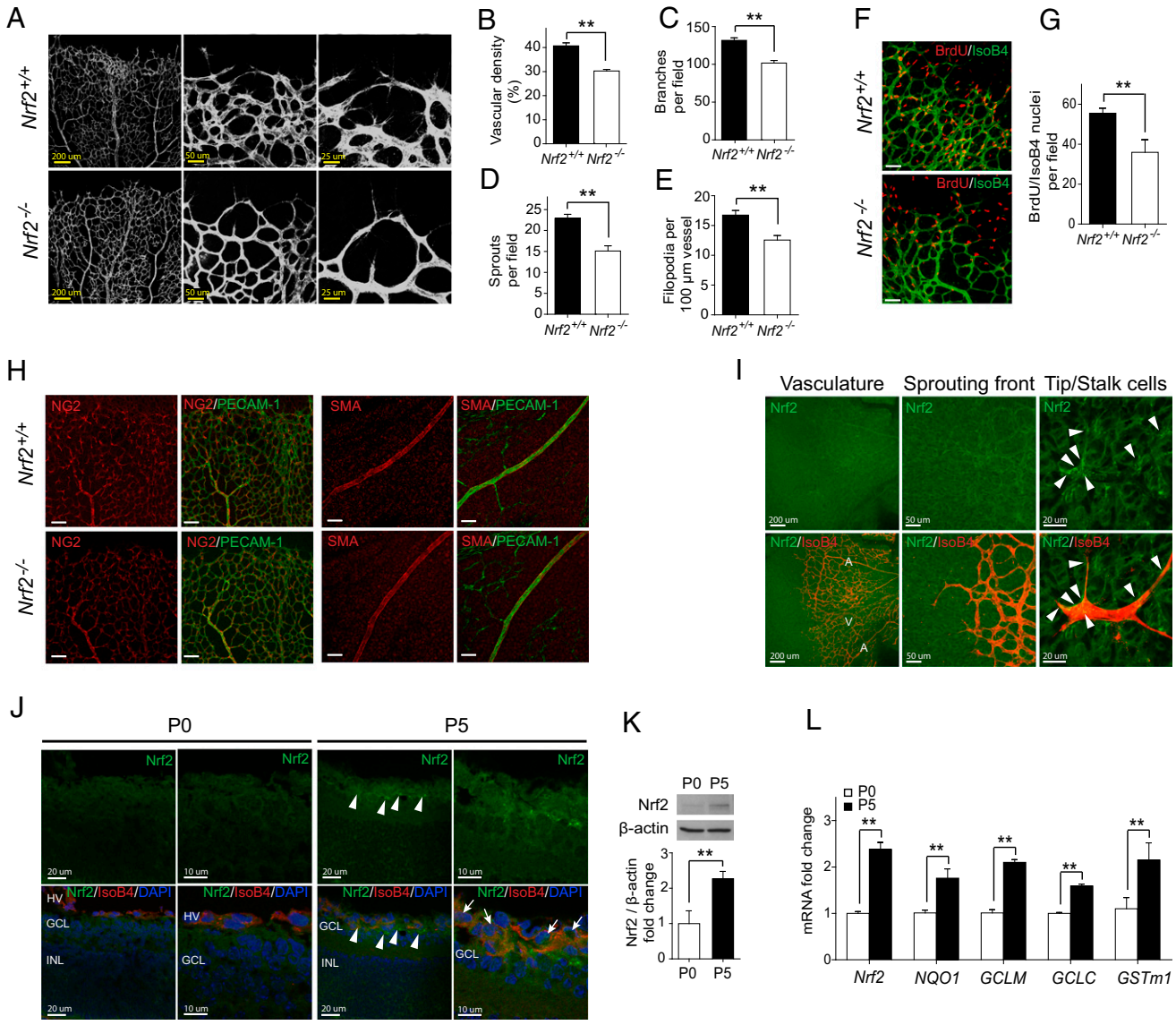

Fig. 1. Genetic ablation of Nrf2 reduces angiogenic sprouting and vascular density. (*A*) Blood vessels were visualized by PECAM-1 staining of retinas at P5. Decreased vascular density (*B*), branch points (*C*), sprouts (*D*), and filopodia (*E*) were observed in $Nrf2^{-/-}$ retina ($n = 6$). (*F* and *G*) Isolectin B4 (green) and BrdU labeling (red) of retinas at P5 demonstrate reduced EC proliferation in $Nrf2^{-/-}$ ($n = 4$). (Scale bar, 50 µm.) (*H*) $NG2^+$ pericytes in capillaries or SMA^+ vascular smooth muscle cells in arterioles were indistinguishable between WT ($Nrf2^{+/+}$) and $Nrf2^{-/-}$ retinas at P5. (Scale bar, 100 µm.) (*I*) Nrf2 is expressed in developing blood vessels, and strong expression was observed in the sprouting vascular front. Arrowheads indicate Nrf2 expression in tip cells and stalk cells (A, artery; V, vein). (*J*) Nrf2 expression was increased in the ganglion cell layer (GCL) of retina at P5 compared with P0. Nrf2 was highly expressed in the vessels and surrounding area (arrowheads). Nrf2 localization in the nucleus was apparent (arrows). HV, hyaloid vessels; INL, inner nuclear layer. (*K*) Immunoblot analysis of Nrf2 in the retinas of WT mice at P0 and P5. β-Actin was used as a loading control ($n = 3$). (*L*) Quantitative RT-PCR analysis of *Nrf2* and Nrf2 target genes in the retinas of WT mice at P0 and P5 ($n = 5$). Data are presented as mean ± SEM (**$P < 0.01$).

(BrdU/IsoB4 positive) in $Nrf2^{-/-}$ retina compared with wild-type (WT) (Fig. 1 *F* and *G*). $NG2^+$ pericytes in capillaries or smooth muscle actin $(SMA)^+$ vascular smooth muscle cells in arterioles were indistinguishable between WT and $Nrf2^{-/-}$ retinas (Fig. 1*H*).

Nrf2 Is Induced and Activated in the Developing Retina. We then examined Nrf2 localization and expression in retinal vessels. Nrf2 expression was found in arteries, veins, and capillaries by retinal whole-mount staining. Strong Nrf2 expression was observed at the vascular leading front, including tip and stalk cells (Fig. 1*I*). Nrf2 was faintly expressed in WT retina at birth (i.e., P0; Fig. 1 *J* and *K*) before retinal vascular development. At P5, increased Nrf2 protein was observed in developing vessels and surrounding retinal tissue, including nuclear localization. (Fig. 1 *J* and *K*). Quantitative PCR (qPCR) results demonstrated significant up-regulation of *Nrf2* and Nrf2 target gene expression (Fig. 1*L*), confirming increased *Nrf2* expression and activity in the developing retina.

***Nrf2* Regulates Angiogenic Sprouting in an EC-Autonomous Manner.** To investigate whether EC-intrinsic Nrf2 regulates sprouting angiogenesis in vivo, we obtained EC-specific KO mice [$Nrf2^{flox/flox}$ ($Nrf2^{fl/fl}$);*Cdh5-Cre*] by mating $Nrf2^{fl/fl}$ with *VE-Cadherin-Cre* mice. *Cdh5*-Cre has been previously demonstrated to attain a recombination efficiency of 88% in retinal vasculature ECs (12). Similar to $Nrf2^{-/-}$, $Nrf2^{fl/fl}$;*Cdh5-Cre* mice exhibited reduced sprouting angiogenesis characterized by decreased number of tip cells, filopodia, branch points, and vascular density (Fig. 2 *A*–*E*).

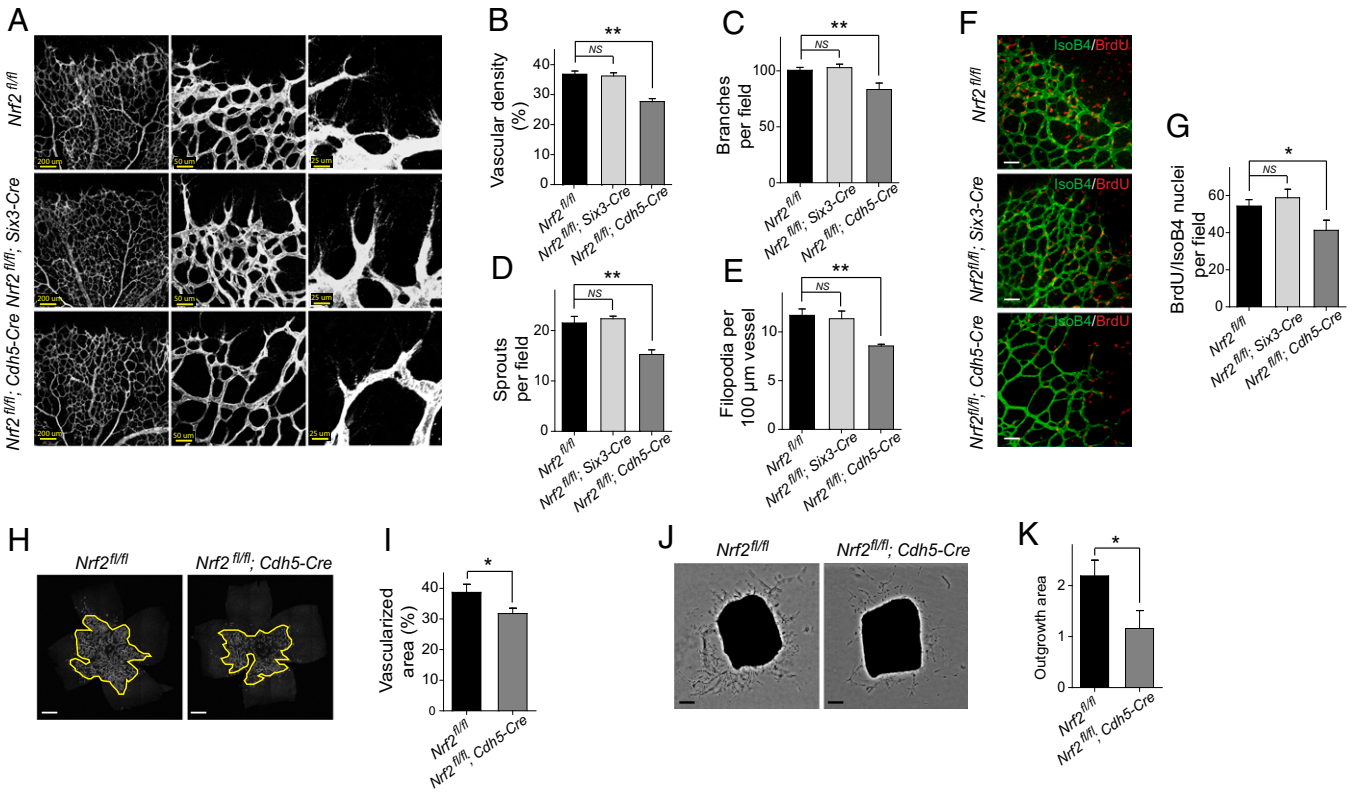

Fig. 2. Nrf2 regulates angiogenic sprouting in an EC-autonomous manner. (*A*) Blood vessels were visualized by PECAM-1 staining of retinas at P5. Decreased vascular density (*B*), branch points (*C*), sprouts (*D*), and filopodia (*E*) were observed in mice with loss of Nrf2 in ECs (i.e., *Nrf2*$^{fl/fl}$;*Cdh5-Cre*), whereas no change in retinal vasculature was observed in mice with loss of Nrf2 in nonvascular retinal tissue (i.e., *Nrf2*$^{fl/fl}$;*Six3-Cre*) compared with control (*Nrf2*$^{fl/fl}$) at P5 (n = 6). (*F* and *G*) Isolectin B4 (green) and BrdU labeling (red) of retinas at P5 demonstrate reduced EC proliferation in *Nrf2*$^{fl/fl}$;*Cdh5-Cre* (*n* = 4). (Scale bar, 50 µm.) (*H* and *I*) Decreased area of the deep vascular plexus was observed in *Nrf2*$^{fl/fl}$;*Cdh5-Cre* retina at P9 (*n* = 6). (Scale bar, 500 µm.) (*J* and *K*) Decreased outgrowth of aortic ring explants from *Nrf2*$^{fl/fl}$;*Cdh5-Cre* (*n* = 6). (Scale bar, 200 µm.) Data are presented as mean ± SEM (*$P < 0.05$; NS, not significant).

There was no change in length of vascular extensions (Fig. S1*B*). To study the effects of Nrf2 in nonvascular tissue on retinal vascular development, we crossed *Nrf2*$^{fl/fl}$ with *Six3-Cre* transgenic mice (13). Cre activity in retina from *Six3-Cre* mice was verified by crossing with *Rosa26-mTmG* reporter mice (14) (Fig. S1 *C*–*Q*) and confirmed Cre expression in retinal neurons and glia, but not blood vessels. In contrast to *Nrf2*$^{fl/fl}$;*Cdh5-Cre*, *Nrf2*$^{fl/fl}$;*Six3-Cre* did not lead to significant changes in retinal vascularization at P5 (Fig. 2 *A*–*E*). A reduction in BrdU^{+} ECs was observed in *Nrf2*$^{fl/fl}$;*Cdh5-Cre* retina, whereas deletion of *Nrf2* in nonvasculature (*Nrf2*$^{fl/fl}$;*Six3-Cre*) did not cause significant changes in the number of proliferating EC (Fig. 2 *F* and *G*). Similar to superficial vasculature, growth of the deep vascular plexus was suppressed in *Nrf2*$^{fl/fl}$;*Cdh5-Cre* retina at P9 (Fig. 2 *H* and *I*). In addition, aortic rings from *Nrf2*$^{fl/fl}$;*Cdh5-Cre* mice displayed reduced sprouting with decrease in EC outgrowth area (Fig. 2 *J* and *K*), compared with corresponding control mice. These results strongly suggest an EC-autonomous function of Nrf2 in the regulation of sprouting angiogenesis.

Deletion of Endothelial Nrf2 Leads to Aberrant Activation of Dll4/Notch Signaling. We assessed VEGF protein levels in developing retinas to determine whether the reduced angiogenesis from deletion of *Nrf2* could be attributed to the changes in VEGF expression. Surprisingly, changes in VEGF expression did not correlate with the vascular phenotypes. Sprouting angiogenesis decreased in *Nrf2*$^{-/-}$ retina, whereas VEGF expression was unaffected. In contrast, *Nrf2*$^{fl/fl}$;*Cdh5-Cre* mice exhibited restrained sprouting angiogenesis, whereas VEGF protein levels were increased in developing retina (Fig. 3 *A*–*C*).

Given the critical role of Dll4 in regulating angiogenic sprouting, we hypothesized that Dll4/Notch signaling might be modulated by Nrf2 deletion. WT (functional) *Nrf2* was absent in *Nrf2*$^{-/-}$ retina (Fig. S2*A*). *Dll4* and Notch target gene (*Nrarp*, *Hes1*, and *Hey1*) expression was higher in *Nrf2*$^{-/-}$ retina compared with WT at P5 (Fig. 3*D*). Interestingly, despite a slight increase in *Dll4* mRNA, only one of three assessed Notch target genes was differentially expressed in *Nrf2*$^{fl/fl}$;*Six3-Cre* retina compared with control (Fig. 3*E*). WT *Nrf2* was decreased in laser-capture microdissected vessels from *Nrf2*$^{fl/fl}$;*Cdh5-Cre* retina (Fig. S2*D*), whereas expression of *Dll4*, *Nrarp*, *Hes1*, and *Hey1* were all significantly increased compared with control (Fig. 3*F*). Immunofluorescence studies demonstrated increased Dll4 expression in the vascular leading front in both *Nrf2*$^{-/-}$ (Fig. S2*E*) and *Nrf2*$^{fl/fl}$;*Cdh5-Cre* retina (Fig. 3*G*) compared with corresponding control. Therefore, EC-intrinsic Nrf2 negatively regulates Dll4/Notch signaling in retinal vascular development.

Inhibition of Dll4/Notch Signaling Abrogates the Restrained Sprouting Angiogenesis in *Nrf2*-Deficient Mice. We next sought to determine whether the restrained sprouting angiogenesis in *Nrf2*-deficient mice could be attributed to the aberrant increase in Dll4 and Notch signaling. To address this, we analyzed whether blockage of Dll4/Notch signaling would restore sprouting angiogenesis in *Nrf2* mutants. The administration of neutralizing Dll4 antibody or γ-secretase inhibitor N-[N-(3,5-difluorophenacetyl-L-alanyl)]-S-phenylglycine t-butyl ester (DAPT) resulted in a hyperdense and hyperbranched vasculature in WT retina 24 h after treatment as previously reported (15) (Fig. 4 *A* and *C*). Discrepancy of vessel density between WT and *Nrf2*$^{-/-}$ was corrected by

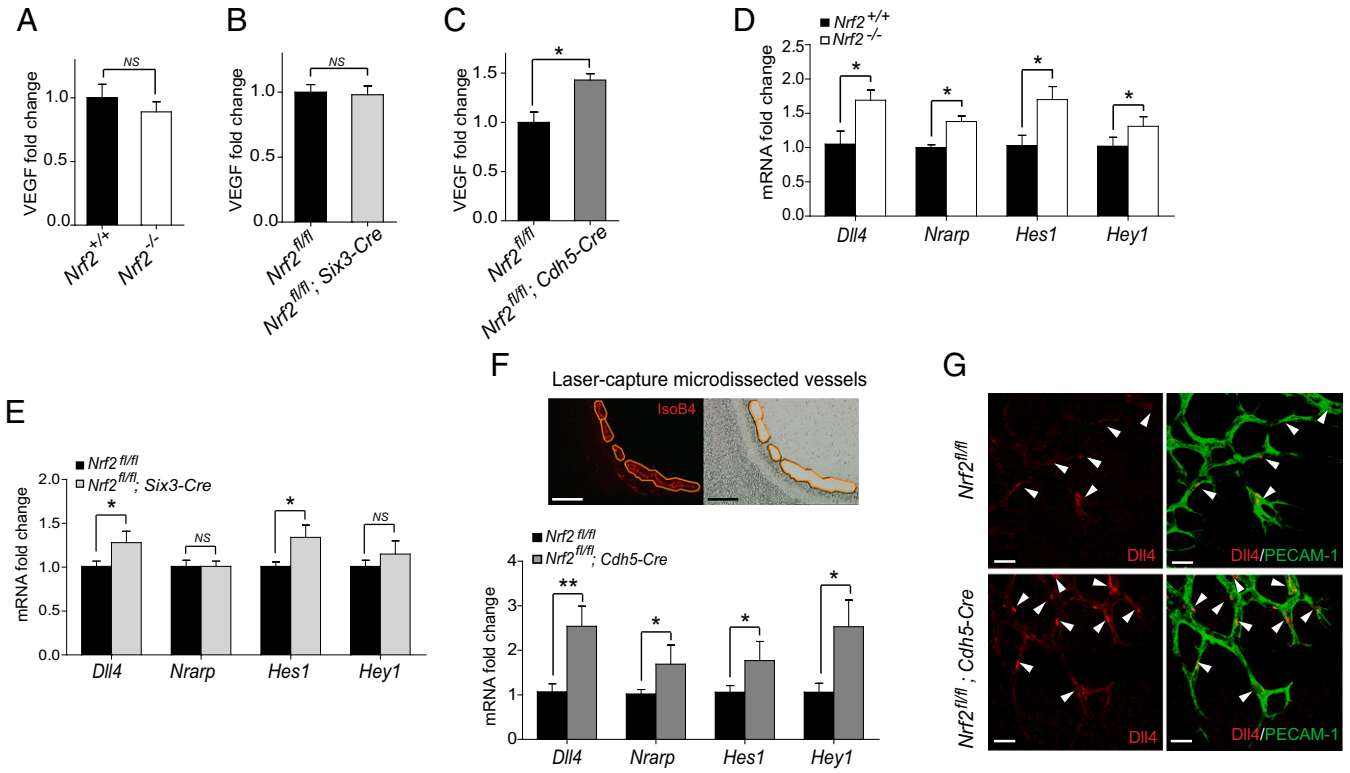

Fig. 3. Deletion of endothelial Nrf2 leads to increased Dll4/Notch signaling. (*A–C*) VEGF protein levels at P5 ($n = 5$). (*D*) Quantitative RT-PCR analysis of *Dll4* and Notch target genes in the retinas of $Nrf2^{-/-}$ and WT mice at P5 ($n = 4$). (*E*) Quantitative RT-PCR analysis of *Dll4* and Notch target genes in the retinas of $Nrf2^{fl/fl}$;*Six3-Cre* and control mice at P5 ($n = 6$). (*F*, *Upper*) Laser-capture microdissection of blood vessels. (Scale bar, 100 μm.) (*F*, *Lower*) Quantitative RT-PCR analysis of *Dll4* and Notch target genes in laser-capture microdissected blood vessels from $Nrf2^{fl/fl}$;*Cdh5-Cre* and control retinas at P5 ($n = 5$). (*G*) Increased Dll4 expression was observed in the angiogenic front (arrowheads) in $Nrf2^{fl/fl}$;*Cdh5-Cre* retinas compared with control at P5. (Scale bar, 25 μm.) Data are presented as mean ± SEM (*$P < 0.05$ and **$P < 0.01$; NS, not significant).

treatment of Dll4 antibody or DAPT, resulting in a similar degree of vessel density in $Nrf2^{-/-}$ and control retina (Fig. 4 *A–D*). We also performed similar pharmacologic inhibition studies with the ex vivo aortic ring assay. Supplementation of neutralizing Dll4 antibody or DAPT in culture medium completely abrogated the reduction of EC outgrowth area of $Nrf2^{fl/fl}$;*Cdh5-Cre* aortic rings (Fig. 4 *E* and *F*). These data confirm that the reduced vascular sprouting and density in mice with loss of endothelial Nrf2 is the consequences of increased Dll4/Notch signaling.

Deletion of the Nrf2 Repressor *Keap1* in ECs Promotes Sprouting Angiogenesis. In light of the vascular phenotype of *Nrf2*-deficient mice, we postulated that Nrf2 GOF in ECs might enhance sprouting angiogenesis in the developing retina. Transgenic mice with deletion of *Keap1* in ECs ($Keap1^{fl/fl}$;*Cdh5-Cre*) were obtained by mating $Keap1^{flox/flox}$ ($Keap1^{fl/fl}$) mice with *VE-Cadherin-Cre* mice. $Keap1^{fl/fl}$;*Cdh5-Cre* retina exhibited hypersprouting (i.e., greater abundance of tip cells and filopodia), enhanced branching, and increased vascular density at P5 (Fig. 5 *A–E*). BrdU incorporation assay showed increased numbers of proliferative ECs (BrdU/IsoB4 positive; Fig. 5 *F* and *G*). Similar to superficial vasculature, growth of the deep vascular plexus was dramatically increased in $Keap1^{fl/fl}$;*Cdh5-Cre* retina at P9 (more than twofold; Fig. 5 *H* and *I*). In contrast to the results in *Nrf2*-deficient retina, $Keap1^{fl/fl}$;*Cdh5-Cre* retina exhibited decreased levels of VEGF (Fig. S3*A*).

Activation of Endothelial Nrf2 by *Keap1* Knockdown Enhances EC Angiogenic Capacity via Suppression of Dll4/Notch Signaling. Our cell-specific KO studies implicate an EC-autonomous role for Nrf2 activation in the regulation of sprouting angiogenesis. We therefore found it useful to use an in vitro system of retinal ECs to gain further insights into the regulation of cell signaling by Nrf2. Increased Nrf2 expression and activity in human retinal ECs (HRECs) from knockdown of *Keap1* was confirmed by Western blot analysis of Nrf2 and qPCR of Nrf2 target genes (Fig. S3 *B* and *C*). Endothelial growth medium with low concentrations of growth factor was used, as *Keap1* deletion can suppress proliferation under starvation conditions (7). *Keap1* knockdown enhanced HREC tube formation (Fig. 5 *J* and *K*) and spheroid sprouting (Fig. 5 *O* and *P*) in the presence of low and high levels of VEGF. The data indicate that Nrf2 activation enhances VEGF promotion of angiogenesis and sprouting in vitro and further supports the EC-autonomous role of Nrf2.

We next investigated whether Nrf2 promotes the angiogenic phenotype in ECs by modulation of Dll4/Notch signaling. Immunofluorescence studies demonstrated increased Dll4 expression in the vascular leading front in $Keap1^{fl/fl}$;*Cdh5-Cre* retina (Fig. 5*L*). Strikingly, Nrf2 overexpression by infection with Ad-*Nrf2* or Nrf2 activation by *Keap1* knockdown in HRECs resulted in reduced protein levels of Dll4 and cleaved Notch intracellular domain (NICD), the active form of Notch (Fig. S3 *E* and *F*). In addition, expression of *Dll4* and Notch target genes was downregulated by *Keap1* knockdown in HRECs collected from the tube formation assay (Fig. 5*M*). The changes in Dll4/Notch signaling were well correlated with the angiogenic phenotype, further implicating Dll4/Notch signaling in the regulation of angiogenesis by Nrf2.

To dissect a distinct effect of Nrf2 on Notch signaling, we cultured *Keap1* siRNA-transfected HRECs in rDll4-coated plates. *Keap1* knockdown reduced NICD levels in HRECs stimulated with rDll4. In addition, *Keap1* knockdown completely

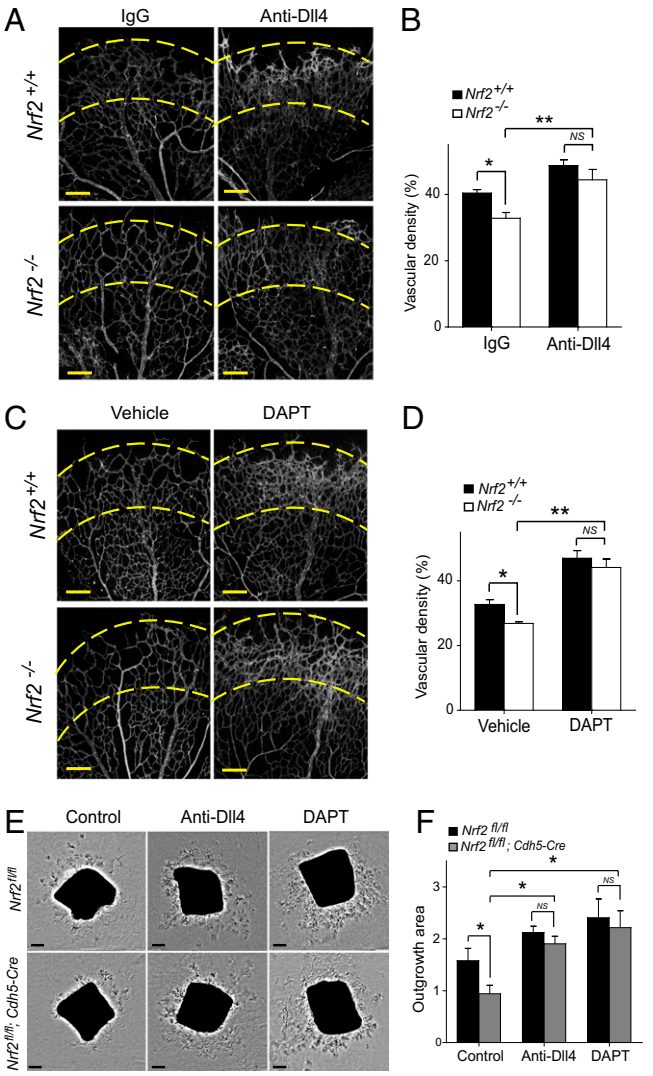

Fig. 4. Inhibition of Dll4/Notch signaling abrogates the restrained sprouting angiogenesis in Nrf2-deficient mice. (*A* and *C*) PECAM-1–stained P5 retina from *Nrf2*$^{-/-}$ and WT mice after 24 h treatment (P4–P5) with Dll4 antibody (intravitreous injection) (*A*) or DAPT (i.p. injection) (*C*). Dll4 antibody or DAPT administration results in comparable vascular hyperplasia in the affected region (between dashed lines) in *Nrf2*$^{-/-}$ and WT retinas. (*B* and *D*) Quantification of vascular density in P5 retinas after 24 h treatment (P4–P5) with Dll4 antibody (intravitreous injection; *B*) or DAPT (i.p. injection; *D*); $n = 6$ per group for Dll4 antibody injection; $n = 5$ per group for DAPT injection. (*E*) Aortic ring explants from *Nrf2*$^{fl/fl}$;*Cdh5-Cre* and control mice treated with Dll4 antibody or DAPT, respectively. (*F*) Quantification of outgrowth area of aortic explants shown in *E* ($n = 7$). (Scale bar, 200 μm.) Data are presented as mean ± SEM (*$P < 0.05$ and **$P < 0.01$; NS, not significant).

abrogated the induction of *Dll4* expression in HRECs cultured on rDll4-coated plates (Fig. 5*N*). The crucial role of Notch signaling in the regulation of sprouting by Nrf2 was further confirmed by Notch inhibition studies with DAPT. When treated with DAPT, control siRNA-transfected HRECs regained sprouting to levels similar to *Keap1* siRNA-transfected HRECs (Fig. 5 *O* and *P*), indicating that Nrf2 regulates EC sprouting via a Notch-dependent mechanism.

Given that hypoxia-inducible factor 2 alpha (HIF-2α) has been implicated in the induction of Dll4 (16), we investigated whether Nrf2 activation affects hypoxia-induced Dll4. Western blotting demonstrated an increased level of hypoxia-inducible factor 1 alpha (HIF-1α), HIF-2α, Dll4, and NICD in control HRECs under hypoxia. *Keap1* knockdown substantially inhibited the induction of HIF-2α, Dll4, and NICD, but accentuated HIF-1α expression (Fig. 5*Q*). The decreased *HIF-2α* mRNA was detected in HRECs with *Keap1* knockdown under hypoxia (Fig. 5*R*) or in blood vessels from *Keap1*$^{fl/fl}$;*Cdh5-Cre* mice (Fig. 5*S*).

Nrf2 Activation Inhibits PI3K/Akt-Dependent Notch Signaling in ECs. Activation of PI3K/AKT plays an essential role in the induction of Dll4/Notch signaling (17–19). We therefore investigated whether PI3K/Akt is involved in the suppression of Dll4/Notch signaling by Nrf2. We found that *Keap1* knockdown totally blocked the induction of PI3K activity by VEGF (Fig. 6*A*). Consistent with effects on VEGF-induced PI3K activity, VEGF-induced phosphorylation of Akt in HRECs was abrogated by *Keap1* knockdown. VEGF-induced VEGFR2 phosphorylation was suppressed by *Keap1* knockdown. In contrast to its effects on Akt, Nrf2 activated Erk. Phosphorylated Erk was surprisingly induced in *Keap1* siRNA-treated HRECs in the absence of VEGF, whereas comparable levels of phospho-Erk were observed in control siRNA- and *Keap1* siRNA-transfected HRECs in the presence of VEGF (Fig. 6*B*). Decreased phospho-Akt was observed in lung and retina from *Keap1*$^{fl/fl}$;*Cdh5-Cre* mice. Western blotting also showed decreased Dll4 and NICD protein in lung from *Keap1*$^{fl/fl}$;*Cdh5-Cre* mice (Fig. 6*C*). PI3K inhibition with LY294002 significantly reduced *Dll4* and *Hey1* expression in control siRNA-treated HREC to a comparable level to that of *Keap1* siRNA treatment (Fig. 6 *D* and *E*). To further implicate the involvement of Akt in Dll4/Notch signaling, we infected HRECs with adenovirus encoding a constitutively active mutant of Akt. Reduction in the expression of Dll4 and NICD in HRECs by *Keap1* knockdown was largely reversed by adenovirus-mediated enhancement of Akt activity (Fig. 6*F*). Taken together, these results suggest that Nrf2 inhibition of Dll4/Notch signaling by Nrf2 in sprouting angiogenesis is, at least partially, ascribed to the suppression of PI3K/Akt.

Discussion

The present study identifies Nrf2 as an essential regulator in sprouting angiogenesis. Nrf2 is significantly increased and activated during vascular development. Deficiency of *Nrf2* in ECs suppresses angiogenic sprouting, whereas constitutive activation of Nrf2 in ECs promotes hypersprouting and vascular density. Strikingly, deficiency of *Nrf2* in the nonvascular retinal cells had no appreciable effect on vascular sprouting, further highlighting the EC-autonomous role of Nrf2. Modulation of Dll4/Notch signaling by Nrf2 appears to be critical for the increase in sprouting angiogenesis. Nrf2 activation by release from Keap1 blocks VEGF-induced VEGFR2-PI3K/Akt in ECs, which may serve as a major mechanism for Nrf2 inhibition of Dll4 and Notch signaling. Under hypoxia, suppression of HIF-2α by Nrf2 activation could be an independent mechanism for the decreased Dll4 expression in ECs (Fig. 6*G*).

In tumor angiogenesis, Nrf2 in cancer cells plays an important role in HIF-1α–dependent VEGF expression (20), and suppression of Nrf2 leads to a reduction of VEGF and blood vessel formation in a mouse xenograft setting (9). In our study, ablation of Nrf2 in the nonvascular retina had no appreciable effect on VEGF levels or vascular sprouting. The results suggest a distinct role of Nrf2 in regulating physiological angiogenesis. In retinal vascular development, VEGF levels were influenced by Nrf2 status in ECs, in a manner that suggested an Nrf2-dependent feedback mechanism. We speculate that increased Notch signaling in *Nrf2*-deficient ECs might reduce responses to VEGF and therefore elicit up-regulation of *VEGF*. Conversely, decreased Notch signaling in *Nrf2*-overexpressing ECs might enhance VEGF response and lead to a down-regulation of *VEGF*. Strikingly, we observed no changes in VEGF expression in either *Nrf2*$^{-/-}$ or *Nrf2*$^{fl/fl}$;*Six3-Cre* retina, indicating that the feedback

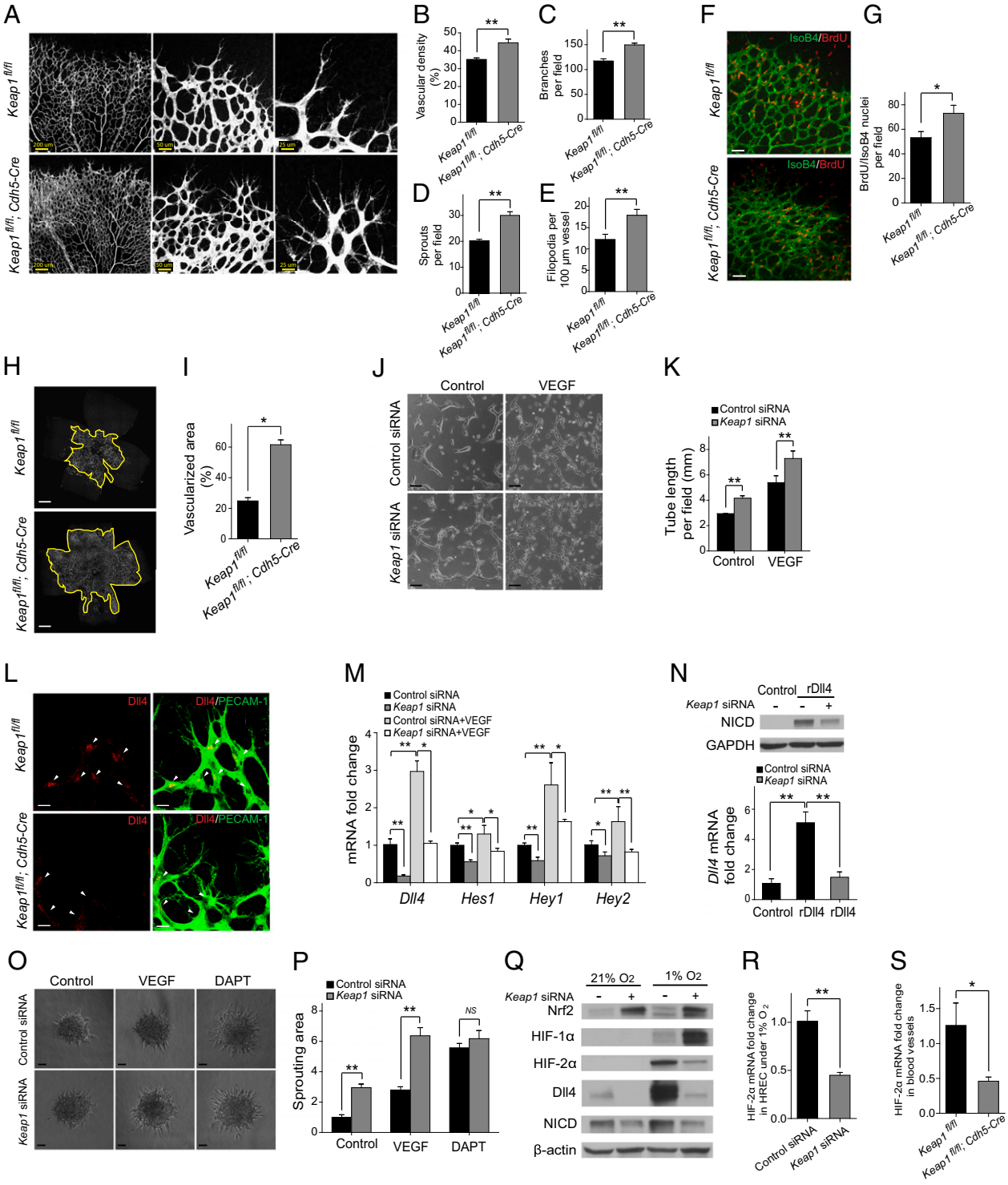

Fig. 5. Deletion of the Nrf2 repressor *Keap1* in ECs promotes sprouting angiogenesis via suppression of Dll4/Notch signaling. (*A*) Visualization of blood vessels by PECAM-1 staining of control (*Keap1*$^{fl/fl}$) and *Keap1*$^{fl/fl}$;*Cdh5-Cre* retinas at P5. Enhanced vascular density (*B*), branch points (*C*), and hypersprouting characterized by increased tip cell numbers (*D*) and filopodia (*E*) were observed in *Keap1*$^{fl/fl}$;*Cdh5-Cre* retina ($n = 6$). (*F* and *G*) Isolectin B4 (green) and BrdU labeling (red) of control and *Keap1*$^{fl/fl}$;*Cdh5-Cre* retinas at P5 ($n = 4$). (Scale bar, 50 µm.) (*H* and *I*) Increased area of the deep vascular plexus was observed in *Keap1*$^{fl/fl}$;*Cdh5-Cre* retina at P9 ($n = 6$). (Scale bar, 500 µm.) (*J* and *K*) *Keap1* knockdown enhanced HREC tube formation. (Scale bar, 100 µm.) (*L*) Increased Dll4 expression was observed at the angiogenic front (arrowheads) in *Nrf2*$^{fl/fl}$;*Cdh5-Cre* retinas at P5. (Scale bar, 25 µm.) (*M*) Quantitative RT-PCR analysis of *Dll4* and Notch target genes in HRECs cultured in a collagen-sandwich gel. (*N*) Immunoblot analysis of NICD and quantitative RT-PCR analysis of *Dll4* in HRECs stimulated with rDll4. GAPDH was detected as a loading control. (*O* and *P*) *Keap1* knockdown enhanced HREC spheroid sprouting with lower or higher level of VEGF. DAPT corrected the differential sprouting between control siRNA and Keap1 siRNA-transfected HRECs. (Scale bar, 50 µm.) (*Q*) Immunoblot analysis of Nrf2, HIF-1α, HIF-2α, Dll4, and NICD in HRECs under normoxia or hypoxia. (*R* and *S*) Quantitative RT-PCR analysis of *HIF-2α* in HRECs under hypoxia (*R*) or in blood vessels (*S*) from *Keap1*$^{fl/fl}$;*Cdh5-Cre* mice at P5 ($n = 4$). Data are presented as mean ± SEM (*$P < 0.05$ and **$P < 0.01$; NS, not significant).

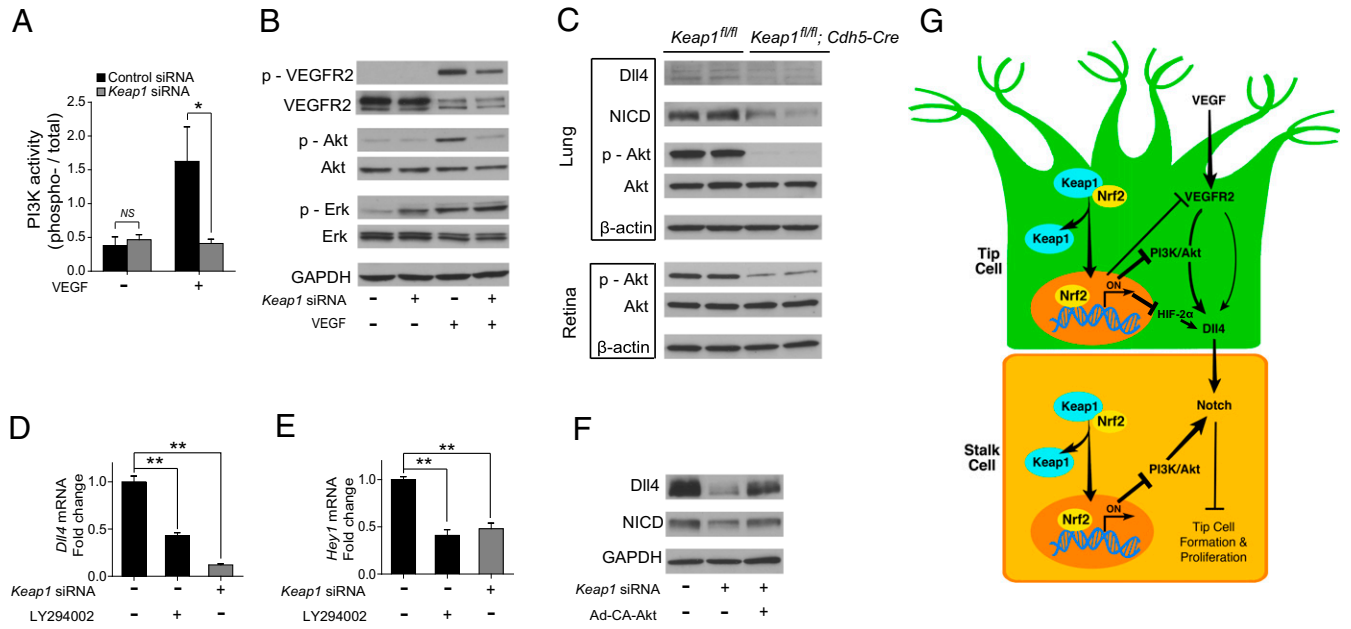

Fig. 6. Nrf2 activation by *Keap1* knockdown inhibits PI3K/Akt-dependent Notch signaling in ECs. (*A*) PI3K activity in HRECs. Knockdown of *Keap1* blocked VEGF-induction of PI3K activity. (*B*) Immunoblot analysis of VEGFR2, Akt, and Erk in HRECs transfected with control siRNA or *Keap1* siRNA in the presence or absence of VEGF. Knockdown of *Keap1* inhibited VEGF-induced phosphorylation of VEGFR2 and Akt, but not Erk. (*C*) Immunoblot analysis of Dll4, NICD, Akt in lung or retina homogenates from *Keap1*$^{fl/fl}$;*Cdh5-Cre* mice at P5. (*D* and *E*) Quantitative RT-PCR analysis of *Dll4* (*D*) and *Hey1* (*E*) in HRECs treated with PI3K inhibitor LY294002. (*F*) Immunoblot analysis of Dll4 and NICD in HRECs expressing constitutively active Akt. Suppression of Dll4 and NICD by *Keap1* knockdown was reversed by adenovirus-mediated enhancement of Akt activity. GAPDH was detected as a loading control. (*G*) Proposed schematic of Nrf2 in developmental angiogenesis. Nrf2 activation by release from Keap1 suppresses Dll4/Notch signaling via inhibition of VEGF-induced VEGFR2-PI3K/Akt and down-regulation of HIF-2α, leading to the enhanced sprouting angiogenesis. Data are presented as mean ± SEM (*$P < 0.05$ and **$P < 0.01$; NS, not significant).

expression of VEGF in tissues surrounding the developing vasculature is Nrf2-dependent. These results suggest that Nrf2 in nonvascular retina is not required for physiological sprouting angiogenesis, and imply a crucial role of EC-intrinsic Nrf2 in deciding the fate of vascular development.

The finding that nonvascular Nrf2 does not affect vascular sprouting in the retina allows the retinal vasculature to be used as an in vivo model for investigating the specific role of EC-intrinsic Nrf2 in sprouting angiogenesis. We found compromised sprouting angiogenesis in *Nrf2*$^{-/-}$ mice in the developing retinal vasculature, which is consistent with a previous study that showed defects in the deep vascular network in *Nrf2*$^{-/-}$ retina (21). Similar to the superficial vasculature, the deep retinal vasculature is also thought to form by sprouting angiogenesis (22). We found that this critical role of Nrf2 in sprouting angiogenesis is EC-autonomous. A previous cell culture study suggested an essential role of Nrf2 in maintenance of EC angiogenic capacity. Knockdown of *Nrf2* or overexpression of *Keap1* impaired proliferation, migration, and tube formation in cultured coronary arterial ECs (23). Our studies demonstrate the proangiogenic ability of EC-intrinsic Nrf2 in vivo, as well as its specific effect on sprouting.

Strikingly, we identified restrained Dll4/Notch signaling by activation of endothelial Nrf2, which contributes to enhancement of vascular sprouting at the angiogenic front. The retinal vascular phenotype we observed with Nrf2 activation in the *Keap1* KO mice is similar to that found in *Dll4*$^{+/-}$ mice (15, 24, 25), in which hypersprouting was observed with no effect on the length of vascular extensions. In our study, the compromised sprouting resulting from Nrf2 deficiency could be rescued by blocking Dll4 or inhibiting Notch activity in vivo, ex vivo, and in vitro, which further confirms the involvement of Dll4/Notch signaling in regulation of angiogenesis by Nrf2. Moreover, constitutively active Nrf2 suppressed Dll4-induced Notch activation, suggesting that Nrf2 might directly inhibit Notch activity in addition to targeting Dll4. The inhibition of Notch exacerbated Dll4 reduction, which contributes to spreading and synchronized suppression of Notch signaling in ECs (26). Interestingly, an in vitro study has reported the binding of Nrf2 to the antioxidant response element in the Notch1 promoter, with up-regulation of Notch1 in liver and mouse embryonic fibroblasts (27). This up-regulation is opposite to the down-regulation we found in ECs, suggesting that the role of Nrf2 in regulating Notch signaling may be cell type-dependent.

VEGF–VEGFR2 signaling plays an essential role in the activation of Dll4/Notch (28). We observed inhibition of VEGF-induced phosphorylation of VEGFR2 and PI3K/Akt, but not Erk, in ECs with constitutively active Nrf2. Previous work has demonstrated that PI3K/AKT positively regulates Dll4/Notch signaling, and the induction of Dll4 expression and Notch signaling is abrogated by blockade of PI3K/Akt phosphorylation (17–19). We therefore postulated that the inhibition of PI3K/Akt by Nrf2 activation might contribute to the suppression of Dll4/Notch that we observed in ECs. This was supported by decreased expression of Dll4 and Notch target genes in ECs treated with PI3K inhibitor, and restoration of Dll4 protein levels and Notch activity in ECs expressing constitutively active Akt. Cross-talk between the Keap1/Nrf2 pathway and PI3K/Akt pathway has been reported in several studies. Nrf2 has been shown to be activated via phosphorylation by PI3K/Akt (29), and pharmacological activation of Nrf2 leads to inhibition of Akt phosphorylation in cancer cells (30–32) and myofibroblasts (33). Our data reveal a critical role of Nrf2 in the regulation of PI3K/Akt activity in ECs, conferring enhanced angiogenic capacity.

The importance of PI3K/Akt as a mediator of Nrf2 regulation of Dll4/Notch is supported by the currently available studies

investigating Akt GOF and LOF in ECs by using adenovirus-mediated gene transfer of Akt mutants. Akt GOF in ECs resulted in increased levels of Dll4 and Notch signaling and target gene expression (17, 19), similar to our findings with Nrf2 LOF in ECs. Conversely, Akt LOF exhibited reduction in Dll4 and Notch signaling (17), similar to our findings with Keap1 LOF and Nrf2 GOF.

We observed distinct, contrasting patterns of Akt and Erk phosphorylation in ECs after Keap1 inactivation. Under basal conditions, *Keap1*-deficient ECs (with constitutively active Nrf2) exhibit enhanced Erk phosphorylation, which could serve to promote EC proliferative capacity. With VEGF stimulation, Keap1-deficient ECs exhibit suppression of PI3K/Akt, which serves to promote angiogenic capacity via suppression of Dll4/Notch. These results suggest a complex role of Nrf2 in the regulation of VEGFR2 signaling in ECs.

Materials and Methods

Animals. The *Nrf2*$^{-/-}$, *Nrf2*$^{fl/f}$, and *Keap1*$^{fl/fl}$ mice have been described previously (34, 35). *VE-Cadherin-Cre* mouse was obtained from Jackson Laboratory and *Six3-Cre* mouse was a gift from Yasuhide Furuta (M. D. Anderson Cancer Center, Houston, TX). Mice were used in accordance with protocols approved by the Institutional Animal Care and Use Committee of The Johns Hopkins University School of Medicine.

Whole-Mount Immunofluorescence Staining and BrdU labeling. Whole-mount Nrf2 staining was performed by using the Mouse on Mouse (M.O.M.) Fluorescein Kit (Vector Laboratories). Alexa-conjugated isolectin GS-IB$_4$ from *Griffonia simplicifolia* (1:150; Invitrogen) was used for vessel staining. Staining with secondary antibody only was used as a negative control (Fig. S1*R*). Retinal platelet/endothelial cell adhesion molecule 1 (PECAM-1) and Dll4 staining was performed as previously described (36). The following primary antibodies were used: monoclonal mouse anti-Nrf2 (5 ng/μL; R&D Systems), monoclonal rat anti-mouse PECAM-1(1:50; BD Pharmingen), and polyclonal goat anti-mouse Dll4 (15 ng/μL; R&D Systems). BrdU labeling was performed as previously described (37) with minor modification. BrdU (Invitrogen) was injected at 300 μg per pup intraperitoneally 2 h before euthanasia. Following isolectin staining, retinas were refixed, washed, and incubated in HCl. BrdU was detected by using Alexa 594-conjugated anti-BrdU mouse monoclonal antibody (Invitrogen). Fluorescently stained retinas were analyzed by a laser scanning microscope (model 710; Zeiss).

Quantitative Analysis. The vessel area density in postnatal mouse retinas was calculated as previously described (38). Relative vascular density was determined by measuring PECAM-1–positive surface area in relation to the total vascularized area. By using the same micrographs, the number of branch points per field was quantified as previously described (25). The point where three capillary segments met was counted as one branch. The number of sprouts and the number of endothelial filopodia per 100-μm vessel length were counted at the sprouting vascular front as previously described (39). For each retina, 10 to 14 random fields were selected to analyze. The quantification was performed by using ImageJ software in a masked fashion.

Cryosection Immunofluorescence Staining. Eyeballs were enucleated and directly embedded in optimal cutting temperature medium (Sakura Finetek) at −80 °C. Cryosection Nrf2 staining was performed by using the M.O.M. Fluorescein Kit. Stained samples were visualized by using a laser scanning microscope (model 710; Zeiss). Staining with secondary antibody only was used as a negative control (Fig. S1*S*).

Laser-Capture Microdissection. Laser-capture microdissection was performed as previously described (40). Vessels were microdissected with the LMD 6000 system (Leica Microsystems) and collected directly into RLT lysis buffer in the RNeasy Micro Kit (Qiagen). Assessments of levels of PECAM-1 (EC marker) and Six3 (marker for non-EC retinal tissue) using real-time PCR confirmed the high purity of microdissected vessels (Fig. S2 *B* and *C*)

Aortic Ring Assay. Aortic ring assay was performed as previously described (41). Aortic rings (1 mm) were cultured in a 1:1 mixture of growth factor reduced Matrigel (BD Bioscience) and EC growth medium-2 (EGM-2; Lonza) for 3 d. The *z*-stack phase-contrast images of the embedded aortas were collected on an Axiovert 200 M microscope (Zeiss).

Cell Cultures. HRECs (Cell Systems) were used at passage <10. For silencing experiments, HRECs were transfected with 25 nM negative control siRNA (catalog no. 4390846; Ambion) or human Keap1 siRNA (catalog no. 4392420; Ambion) by using Lipofectamine 2000 transfection reagent (Invitrogen). Human VEGF (R&D Systems) and LY294002 (Calbiochem) were used for stimulation and PI3K inhibition experiments, respectively. For Nrf2 overexpression, HRECs were infected with control adenovirus (Ad-*GFP*) or adenovirus encoding Nrf2 (Ad-*Nrf2*) as described previously (42). For activation of Akt, HRECs were infected with control adenovirus (Ad-CMV-null, catalog no. 1300; Vector Biolabs) or adenovirus encoding Akt (ca) [Ad-CA-Akt1 (Myr), catalog no. 1020; Vector Biolabs].

Tube Formation Assay. Tube formation assay was performed as previously described (43). Ten random fields displaying tubes in each well were selected for analysis after culture in a collagen-sandwich gel for 24 h. Total tube length per field was quantified by using ImageJ software in a masked fashion. For qPCR analysis, type I collagenase (Worthington Biochemical) was added to dissolve collagen. Cells were collected by centrifugation and subjected to RNA purification by using an RNeasy Mini Kit (Qiagen).

Spheroid Sprouting Assay. The spheroid sprouting assay was performed as previously described (44) with minor modification. Spheroids were seeded into 300-μL collagen solution containing collagen I from rat tail (BD Biosciences) in a 24-well plate. EGM-2 or EGM-2 supplemented with VEGF or DAPT was added to the top of collagen. Five hours later, images were taken by using an Axiovert 200 M microscope (Zeiss). Spheroid sprouting area (10 spheroids per condition) was quantified by using Adobe Photoshop.

PI3K Activity Assay. PI3K activity was assessed by using FACE PI3-kinase p85 ELISA Kit (Active Motif) according to the manufacturer's instructions. Phosphorylated and total PI3K were measured, and results were normalized to cell number.

Chemical Interventions. To inhibit Dll4-Notch signaling, purified anti-mouse Dll4 antibody (BioLegend) or DAPT (Sigma-Aldrich; dissolved in DMSO) were used. To induce Notch signaling, plates were coated with human recombinant Dll4 (1 μg/mL; R&D Systems).

qPCR. Total RNA isolation from retina and reverse transcription were performed as previously described (34). For laser-capture microdissected vessels, total RNA was purified by using the RNeasy Micro Kit (Qiagen). cDNA was synthesized using the iScript cDNA Synthesis Kit (Bio-Rad). Real-time PCR was performed by using SYBR Premix Ex Taq (Takara) with a Stratagene Mx3005P qPCR system (Agilent Technologies). Primers for Nrf2 were designed to amplify exon 5, to allow differentiation between WT (functional) Nrf2 and the mutated Nrf2 in the KO mice. Results from retina or ECs were normalized by cyclophilin A or GAPDH, respectively.

Western Blot. Western blot was performed as previously described (36). The following antibodies were used: rabbit anti-Nrf2, mouse anti-GAPDH (Abcam), rabbit anti–β-actin, rabbit anti-NICD, rabbit anti–phospho-Akt, mouse anti-Akt1, mouse anti–phospho-p44/42 MAPK (Erk1/2), rabbit anti-p44/42 MAPK (Erk1/2), and rabbit anti-Dll4 (Cell Signaling Technology).

Statistical Analysis. Results were expressed as mean ± SEM. Data were analyzed by unpaired Student *t* test. *P* values less than 0.05 were considered statistically significant.

ACKNOWLEDGMENTS. We thank Yas Furuta (M. D. Anderson Cancer Center) for *Six3-Cre* mice. We thank Zhenhua Xu and Jerry Lutty (Department of Ophthalmology); Jing Cai (Department of Molecular Biology and Genetics); and Huaqiang Fang (The Solomon H. Snyder Department of Neuroscience) from The Johns Hopkins University School of Medicine for helpful discussions and suggestions. This work was supported by National Institutes of Health Grant EY022683 (to E.J.D.) and a Research to Prevent Blindness Career Development Award (to E.J.D.).

1. Carmeliet P (2005) Angiogenesis in life, disease and medicine. *Nature* 438(7070): 932–936.

2. Gerhardt H, et al. (2003) VEGF guides angiogenic sprouting utilizing endothelial tip cell filopodia. *J Cell Biol* 161(6):1163–1177.

3. Eilken HM, Adams RH (2010) Dynamics of endothelial cell behavior in sprouting angiogenesis. *Curr Opin Cell Biol* 22(5):617–625.
4. Kim J, Oh WJ, Gaiano N, Yoshida Y, Gu C (2011) Semaphorin 3E-Plexin-D1 signaling regulates VEGF function in developmental angiogenesis via a feedback mechanism. *Genes Dev* 25(13):1399–1411.
5. Kensler TW, Wakabayashi N, Biswal S (2007) Cell survival responses to environmental stresses via the Keap1-Nrf2-ARE pathway. *Annu Rev Pharmacol Toxicol* 47:89–116.
6. DeNicola GM, et al. (2011) Oncogene-induced Nrf2 transcription promotes ROS detoxification and tumorigenesis. *Nature* 475(7354):106–109.
7. Mitsuishi Y, et al. (2012) Nrf2 redirects glucose and glutamine into anabolic pathways in metabolic reprogramming. *Cancer Cell* 22(1):66–79.
8. Tsai JJ, et al. (2013) Nrf2 regulates haematopoietic stem cell function. *Nat Cell Biol* 15(3):309–316.
9. Kim TH, et al. (2011) NRF2 blockade suppresses colon tumor angiogenesis by inhibiting hypoxia-induced activation of HIF-1α. *Cancer Res* 71(6):2260–2275.
10. Nijmeh J, Moldobaeva A, Wagner EM (2010) Role of ROS in ischemia-induced lung angiogenesis. *Am J Physiol Lung Cell Mol Physiol* 299(4):L535–L541.
11. Ichihara S, et al. (2010) Ablation of the transcription factor Nrf2 promotes ischemia-induced neovascularization by enhancing the inflammatory response. *Arterioscler Thromb Vasc Biol* 30(8):1553–1561.
12. Economopoulou M, et al. (2009) Histone H2AX is integral to hypoxia-driven neovascularization. *Nat Med* 15(5):553–558.
13. Furuta Y, Lagutin O, Hogan BL, Oliver GC (2000) Retina- and ventral forebrain-specific Cre recombinase activity in transgenic mice. *Genesis* 26(2):130–132.
14. Muzumdar MD, Tasic B, Miyamichi K, Li L, Luo L (2007) A global double-fluorescent Cre reporter mouse. *Genesis* 45(9):593–605.
15. Hellström M, et al. (2007) Dll4 signalling through Notch1 regulates formation of tip cells during angiogenesis. *Nature* 445(7129):776–780.
16. Skuli N, et al. (2012) Endothelial HIF-2α regulates murine pathological angiogenesis and revascularization processes. *J Clin Invest* 122(4):1427–1443.
17. Takeshita K, et al. (2007) Critical role of endothelial Notch1 signaling in postnatal angiogenesis. *Circ Res* 100(1):70–78.
18. Hayashi H, Kume T (2008) Foxc transcription factors directly regulate Dll4 and Hey2 expression by interacting with the VEGF-Notch signaling pathways in endothelial cells. *PLoS ONE* 3(6):e2401.
19. Zhang J, et al. (2011) Angiopoietin-1/Tie2 signal augments basal Notch signal controlling vascular quiescence by inducing delta-like 4 expression through AKT-mediated activation of beta-catenin. *J Biol Chem* 286(10):8055–8066.
20. Zhang Z, et al. (2013) Reactive oxygen species regulate FSH-induced expression of vascular endothelial growth factor via Nrf2 and HIF1α signaling in human epithelial ovarian cancer. *Oncol Rep* 29(4):1429–1434.
21. Uno K, et al. (2010) Role of Nrf2 in retinal vascular development and the vaso-obliterative phase of oxygen-induced retinopathy. *Exp Eye Res* 90(4):493–500.
22. Fruttiger M (2007) Development of the retinal vasculature. *Angiogenesis* 10(2):77–88.
23. Valcarcel-Ares MN, et al. (2012) Disruption of Nrf2 signaling impairs angiogenic capacity of endothelial cells: implications for microvascular aging. *J Gerontol A Biol Sci Med Sci* 67(8):821–829.
24. Suchting S, et al. (2007) The Notch ligand Delta-like 4 negatively regulates endothelial tip cell formation and vessel branching. *Proc Natl Acad Sci USA* 104(9):3225–3230.
25. Lobov IB, et al. (2007) Delta-like ligand 4 (Dll4) is induced by VEGF as a negative regulator of angiogenic sprouting. *Proc Natl Acad Sci USA* 104(9):3219–3224.
26. Caolo V, et al. (2010) Feed-forward signaling by membrane-bound ligand receptor circuit: the case of NOTCH DELTA-like 4 ligand in endothelial cells. *J Biol Chem* 285(52):40681–40689.
27. Wakabayashi N, et al. (2010) Regulation of notch1 signaling by nrf2: implications for tissue regeneration. *Sci Signal* 3(130):ra52.
28. Phng LK, Gerhardt H (2009) Angiogenesis: A team effort coordinated by notch. *Dev Cell* 16(2):196–208.
29. Jeong WS, Jun M, Kong AN (2006) Nrf2: A potential molecular target for cancer chemoprevention by natural compounds. *Antioxid Redox Signal* 8(1-2):99–106.
30. Deeb D, Gao X, Dulchavsky SA, Gautam SC (2007) CDDO-me induces apoptosis and inhibits Akt, mTOR and NF-kappaB signaling proteins in prostate cancer cells. *Anticancer Res* 27(5A):3035–3044.
31. Ling X, et al. (2007) The novel triterpenoid C-28 methyl ester of 2-cyano-3, 12-dioxoolen-1, 9-dien-28-oic acid inhibits metastatic murine breast tumor growth through inactivation of STAT3 signaling. *Cancer Res* 67(9):4210–4218.
32. Liu Y, Gao X, Deeb D, Gautam SC (2012) Oleanane triterpenoid CDDO-Me inhibits Akt activity without affecting PDK1 kinase or PP2A phosphatase activity in cancer cells. *Biochem Biophys Res Commun* 417(1):570–575.
33. Kulkarni AA, et al. (2011) PPAR-γ ligands repress TGFβ-induced myofibroblast differentiation by targeting the PI3K/Akt pathway: Implications for therapy of fibrosis. *PLoS ONE* 6(1):e15909.
34. Wei Y, et al. (2011) Nrf2 has a protective role against neuronal and capillary degeneration in retinal ischemia-reperfusion injury. *Free Radic Biol Med* 51(1):216–224.
35. Kong X, et al. (2011) Enhancing Nrf2 pathway by disruption of Keap1 in myeloid leukocytes protects against sepsis. *Am J Respir Crit Care Med* 184(8):928–938.
36. Xu Z, et al. (2012) MEF2C ablation in endothelial cells reduces retinal vessel loss and suppresses pathologic retinal neovascularization in oxygen-induced retinopathy. *Am J Pathol* 180(6):2548–2560.
37. Benedito R, et al. (2009) The notch ligands Dll4 and Jagged1 have opposing effects on angiogenesis. *Cell* 137(6):1124–1135.
38. Stenzel D, et al. (2011) Endothelial basement membrane limits tip cell formation by inducing Dll4/Notch signalling in vivo. *EMBO Rep* 12(11):1135–1143.
39. Benedito R, et al. (2012) Notch-dependent VEGFR3 upregulation allows angiogenesis without VEGF-VEGFR2 signalling. *Nature* 484(7392):110–114.
40. Joyal JS, et al. (2011) Ischemic neurons prevent vascular regeneration of neural tissue by secreting semaphorin 3A. *Blood* 117(22):6024–6035.
41. Soucy KG, et al. (2010) Single exposure to radiation produces early anti-angiogenic effects in mouse aorta. *Radiat Environ Biophys* 49(3):397–404.
42. Kosmider B, et al. (2012) Nrf2 protects human alveolar epithelial cells against injury induced by influenza A virus. *Respir Res* 13:43.
43. Yoshida T, Gong J, Xu Z, Wei Y, Duh EJ (2012) Inhibition of pathological retinal angiogenesis by the integrin αvβ3 antagonist tetraiodothyroacetic acid (tetrac). *Exp Eye Res* 94(1):41–48.
44. Chen J, et al. (2011) Wnt signaling mediates pathological vascular growth in proliferative retinopathy. *Circulation* 124(17):1871–1881.